A one-step synthesis of an iridium(II) dinuclear complex. Preparation, structures and properties of bis(μ-acetato)-dicarbonyldichlorodiiridium(II) complexes †

Naohiro Kanematsu,[a] Masahiro Ebihara[b] and Takashi Kawamura *[a]

[a] *Department of Chemistry, Faculty of Engineering, Gifu University, Yanagido, Gifu 501-1193, Japan. E-mail: kawamura@apchem.gifu-u.ac.jp*
[b] *Institute for Molecular Science, Myodaiji, Okazaki 444-8585, Japan*

A bis(μ-acetato)dicarbonyldichlorodiiridium(II) complex, $[Ir_2(\mu\text{-}O_2CMe)_2Cl_2(CO)_2]$ **1**, was prepared by a one-step reaction of H_2IrCl_6 with $MeCO_2Li$ under O_2 in a mixed solvent of acetic acid and acetic anhydride. Dissolution of **1** in various ligating solvents gave $[Ir_2(\mu\text{-}O_2CMe)_2Cl_2(CO)_2L_2]$ (L = MeCN **2**, dmso **3**, py **4** or 4-isopropylpyridine **5**). Crystal structure determinations of **2**, **3** and **4** gave the Ir–Ir distances of 2.569(1), 2.5980(5) and 2.5918(5) Å, respectively, which are in the range of reported Ir^{II}–Ir^{II} single-bond distances. CV of **2**, **4** and **5** exhibited a one-electron quasi-reversible oxidation wave at $E_{1/2}$ of 1.30, 0.97 and 0.94 V *vs.* Fc^+–Fc, respectively. Complex **3** gave no CV response in the potential window of dmso. Electrolytic or radiolytic one-electron oxidation of **4** and **5** gave their cationic radicals, of which frozen solutions gave pseudo-axially symmetric ESR spectra. The g tensors $g_1 = 2.62$, $g_2 = 2.49$ and $g_3 = 1.81$ for **4**$^{+\bullet}$ and $g_\perp = 2.51$ and $g_\parallel = 1.82$ for **5**$^{+\bullet}$ suggest that their odd electron is accommodated in the δ_{IrIr}^* orbital.

Introduction

A variety of lantern-type dirhodium(II) complexes has been synthesized and their structures, properties, catalytic activities and electronic structures have been investigated.[1] We reported their electronic configurations based on analysis of ESR spectra of Rh_2^{5+} species and theoretical calculations.[2–6] In these reports we have shown that the symmetry of the odd-electron orbital of Rh_2^{5+} complexes depends on the bridging and axial ligands. Diiridium(II) complexes are expected to have stronger metal–metal and metal–ligand interactions than those of the 3d and 4d metal cluster compounds. However, only a limited number of singly bonded Ir_2^{4+} compounds are known. To our knowledge the structures of ten Ir_2^{4+} complexes with anionic bridging ligands have been reported: the complexes with pyrazolato,[7–11] N,N'-di-p-tolylformamidinato[12–14] and sulfur containing[15,16] bridges. Synthesis of all these Ir_2^{4+} complexes includes oxidation of parent Ir_2^{2+} complexes.

We have tried development of a simple synthetic method for Ir_2^{4+} complexes with bridging acetato ligands which is a classical one for lantern-type dimetal complexes. The acetato-bridged complexes are expected to be useful starting materials to synthesize Ir_2^{4+} complexes with other ligands such as amidates or amidinates. We report here synthesis of a new Ir_2^{4+} complex with two bridging acetato, two chloro and two carbonyl ligands, $[Ir_2(\mu\text{-}O_2CMe)_2Cl_2(CO)_2]$ **1**. Some axial solvent adducts of **1** are also synthesized and their crystal structures and redox properties examined. The electronic structures of some of their cationic radicals are also studied based on ESR.
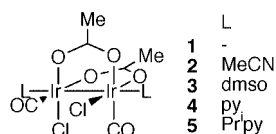
† *Supplementary data available*: rotatable 3-D crystal structure diagram in CHIME format. See http://www.rsc.org/suppdata/dt/1999/4413/

Experimental

^{1}H NMR spectra were recorded on a JEOL α400 or a Varian INOVA 400 spectrometer, IR spectra using a Perkin-Elmer FT IR-1640 spectrophotometer and UV-VIS absorption spectra on a Hitachi U-3500 or a Shimadzu UV-3100PC spectrophotometer. CV Studies were performed with a BAS 50W electrochemical analyzer employing a conventional three-electrode cell with a platinum disk working electrode, a platinum wire counter electrode, and a BAS RE-5 Ag^+–Ag reference electrode. Electrolytic solutions were CH_2Cl_2, dmso, or MeCN containing 0.1 M $Bu^n_4NPF_6$. After each CV measurement the oxidation potential of ferrocene in the same electrolytic solution was measured and the electrode potential converted into that relative to Fc^+–Fc. For coulometry or bulk electrolytic oxidation the working electrode a platinum coil and the counter a gold coil in a two-compartment cell connected by a sintered glass disk. ESR spectra were recorded on a JEOL JES-TE200 spectrometer. Field sweep was monitored with an Echo Electronics EFM-200 ^{1}H NMR gaussmeter. The probe was attached beside the ESR cavity; the field difference between the ESR and the NMR sample positions was calibrated by measuring the field intensity at the resonance of perylene cationic radical in concentrated H_2SO_4 (g = 2.002583).

Syntheses

$[Ir_2(\mu\text{-}O_2CMe)_2Cl_2(CO)_2]$ 1. The compounds $H_2IrCl_6\cdot6H_2O$ (2.78 g, 5.54 mmol) and $MeCO_2Li$ (0.392 g, 5.99 mmol) in a mixed solvent of acetic acid (35 mL) and acetic anhydride (15 mL) were refluxed for 24 h with vigorous bubbling of O_2. The reddish brown precipitate obtained by decantation of the solution was rinsed with CH_2Cl_2 (5 mL) and MeOH (1 mL) and dried *in vacuo*. Yield 0.524 g (30%) (Found: C, 11.53; H, 1.06; Cl, 11.10. $C_3H_3ClIrO_3$ requires C, 11.45; H, 0.96; Cl, 11.26%); δ_H (as $[Ir_2(\mu\text{-}O_2CMe)_2Cl_2(CO)_2(dmso\text{-}d_6)_2]$ in dmso-d_6) 2.19 (s, O_2CCH_3); $\tilde{\nu}_{max}/cm^{-1}$ 2066m, 2031s, 1560s, 1542s, 1508m, 1458m, 1090w, 1010w, 715w and 596w (KBr).

[Ir₂(μ-O₂CMe)₂Cl₂(CO)₂(MeCN)₂] 2. A suspension of complex **1** (138 mg, 0.219 mmol) in MeCN (10 mL) was stirred for 1 h at room temperature. The resulting yellow solution was loaded onto a silica gel column and eluted with MeCN–CH₂Cl₂ (1:1 v/v). The first yellow fraction was dried to give **2** as yellow crystals. Yield 100 mg (64%) (Found: C, 17.14; H, 1.72; Cl, 9.79; N, 4.13. $C_5H_6ClIrNO_3$ requires C, 16.88; H, 1.70; Cl, 9.96; N, 3.94%); δ_H (CD₃CN) 2.16 (s, O₂CCH₃); $\tilde{\nu}_{max}$/cm⁻¹ 2033s, 1654s, 1543s, 1508m, 1450s, 1408m and 715w (KBr); λ_{max}/nm (MeCN) 351 (ε/M⁻¹ cm⁻¹ 12000) and 412 (6700).

[Ir₂(μ-O₂CMe)₂Cl₂(CO)₂(dmso)₂] 3. Dimethyl sulfoxide (0.5 mL) was added to complex **1** (98 mg, 0.16 mmol) suspended in CH₂Cl₂ (4 mL), and the mixture stirred for 1 h. The yellow solution was evaporated to dryness. The residue was purified on a silica gel column by eluting with CH₂Cl₂–dmso (100:1 v/v). The yellow fraction was dried to give **3** as yellow crystals. Yield 52 mg (40%) (Found: C, 15.41; H, 2.19. $C_5H_9ClIrO_4S$ requires C, 15.29; H, 2.31%); δ_H (dmso-d₆) 2.19 (s, O₂CCH₃); $\tilde{\nu}_{max}$/cm⁻¹ 2033s, 1560m, 1535m, 1508w, 1450m, 1420m, 1409m, 1115s, 1015s, 968w, 711w, 578w and 553w (KBr); λ_{max}/nm (dmso) 299 (ε/M⁻¹ cm⁻¹ 29000), 342 sh and 397 sh.

[Ir₂(μ-O₂CMe)₂Cl₂(CO)₂(py)₂] 4. Pyridine (1 mL) was added to complex **1** (46 mg, 0.073 mmol) suspended in toluene (10 mL), and the mixture stirred for 1 h followed by evaporation to dryness. The crude product was purified on a silica gel column by eluting with CH₂Cl₂. The yellow eluent was dried to give **4** as yellow crystals. Yield 46 mg (77%) (Found: C, 24.53; H, 2.10. $C_8H_8ClIrNO_3$ requires C, 24.40; H, 2.05%); δ_H (CD₂Cl₂) 8.81 (d, 4 H, *o*-H of py), 7.99 (t, 2 H, *p*-H of py), 7.58 (t, 4 H, *m*-H of py) and 2.17 (s, 6 H, O₂CCH₃); $\tilde{\nu}_{max}$/cm⁻¹ 2024s, 2003s, 1560s, 1543m, 1508w, 1451s, 1218m, 1070m, 755w, 693w and 634w (KBr); λ_{max}/nm (CH₂Cl₂) 333 sh and 399 (ε/M⁻¹ cm⁻¹ 7600).

[Ir₂(μ-O₂CMe)₂Cl₂(CO)₂(Prⁱpy)₂] 5. A mixture of Prⁱpy (4-isopropylpyridine, 116 mg, 0.96 mmol) and complex **1** (98 mg, 0.16 mmol) in CH₂Cl₂ (20 mL) was stirred for 3 h. The yellow solution was evaporated to dryness. The residual powder was dissolved in CH₂Cl₂ (10 mL), loaded onto a silica gel column and eluted with CH₂Cl₂–hexane (10:1 v/v). The yellow eluent was dried to give **5** as yellow crystals. Yield 106 mg (78%) (Found: C, 30.19; H, 3.24; Cl, 7.85; N, 3.30. $C_{11}H_{14}ClIrNO_3$ requires C, 30.31; H, 3.24; Cl, 8.13; N, 3.21%); δ_H (CDCl₃) 8.70 (d, 4 H, *o*-H of py), 7.38 (d, 4 H, *m*-H of py), 3.02 (sep, 2 H, C*H*Me₂), 2.18 (s, 6 H, O₂CCH₃) and 1.33 (d, 12 H, CH(C*H*₃)₂); $\tilde{\nu}_{max}$/cm⁻¹ 2961m, 2893w, 2863w, 2032s, 2014s, 1970s, 1617s, 1568s, 1544m, 1491w, 1448s, 1429m, 1363w, 1228m, 1068m, 1056m, 1021s, 835m, 713m and 566m (KBr); λ_{max}/nm (CH₂Cl₂) 331 sh and 398 (ε/M⁻¹ cm⁻¹ 7900).

Crystallographic study

Prismatic yellow single crystals of complex **2** were obtained by slow evaporation of its MeCN solution. Slow evaporation of solvent from CH₂Cl₂–PrⁿCN (10:1 v/v) solutions of **3** and **4** gave their yellow single crystals. All measurements were carried out on a Rigaku AFC7R diffractometer with graphite monochromated Mo-Kα radiation (λ = 0.71069 Å). The data were collected by using the ω–2θ scan technique to a maximum 2θ value of 55°. All calculations were performed using TEXSAN.[17] Scattering factors for neutral atoms were from Cromer and Waber[18] and anomalous dispersion[19] was included. Crystal data and details of structure refinement parameters are listed in Table 1. The structures were solved by direct methods SHELXS 86.[20] X-Ray absorption for **2** and **4** was corrected by using DIFABS.[21] An analytical absorption correction[22] was applied for **3**. In the crystal of **4** the complex was on a crystallographic twofold axis and Cl atoms and CO groups are disordered and the occupancy of one set (Cl(1), C(3) and O(3)) was refined as

0.63 and that of the other (Cl(2), C(4) and O(4)) as 0.37. Final full-matrix least-squares cycles included all non-hydrogen atoms with anisotropic thermal parameters and all hydrogen atoms at calculated positions using idealized geometries C–H 0.95 Å with isotropic thermal parameters which were 1.2 times those of the connected atoms.

CCDC reference number 186/1710.

See http://www.rsc.org/suppdata/dt/1999/4413/ for crystallographic files in .cif format.

ESR

By electrolysis. Bulk electrolysis was performed at 258 K at a potential 0.3 V more positive than $E_{1/2}$ for the oxidation in CH₂Cl₂ solution containing 0.1 M BuⁿN₄PF₆ as a supporting electrolyte and *ca.* 10 mM of complex **4** or **5** by using the cell for coulometry. Upon electrolysis the electrolytic solution became green in 15 min and this was quickly transferred to an ESR sample tube and frozen at 77 K.

By radiolysis. A degassed Freon mixture (CH₂Cl₂–CFCl₃–CF₂BrCF₂Br 0.1:5:5, v/v) solution saturated with complex **5** was sealed in an ESR sample tube.[2,23,24] The solution was exposed to X-rays (Mo-Kα, 14.5 kW) at 77 K for 4 h to generate the cationic radical of the solute. The ESR spectrum of the cationic radical was obtained for the irradiated frozen solution after careful annealing to decay the paramagnetic species from the solvent.

Results and discussion

Synthesis

A reddish brown precipitate was formed by the reaction of H₂IrCl₆·6H₂O with MeCO₂Li in a mixture of acetic acid and acetic anhydride with rigorous O₂ bubbling. The precipitate did not dissolve in CH₂Cl₂, CHCl₃ or toluene, but dissolved in MeCN, dmso, py and Prⁱpy. The precipitated reaction product was dissolved in a mixture of CH₂Cl₂ and one of the ligating solvents (L) to give [Ir₂(μ-O₂CMe)₂Cl₂(CO)₂L₂]. Therefore, the reddish brown precipitate is presumed to be an iridium dinuclear complex without axial ligands, [Ir₂(μ-O₂CMe)₂-Cl₂(CO)₂] **1**. Elemental analysis and IR data which showed characteristic bands of terminal CO (2066 and 2031 cm⁻¹) support this. Iridium(II) dinuclear complexes have been synthesized by the oxidation of iridium(I) dinuclear complexes. In the present procedure **1** is prepared by a single step reaction from a commercially available material, H₂IrCl₆·6H₂O.
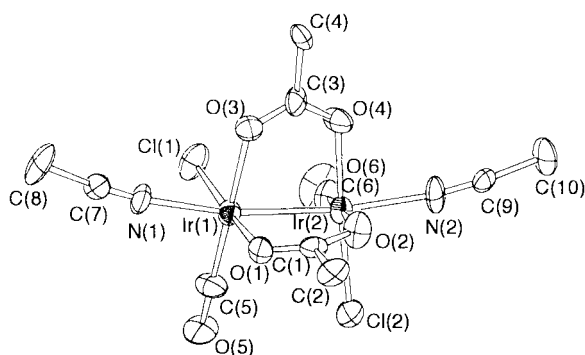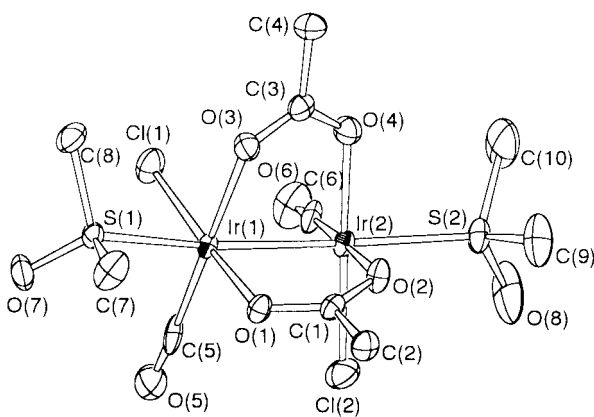
The reaction mechanism for the formation of complex **1** is not a simple reduction but may include more complex reduction and oxidation processes. The yield depends on the rate of bubbling of O₂ gas. Without O₂ gas, a black precipitate was formed which was an unknown iridium carbonyl complex since the IR spectrum showed a strong absorption band of terminal CO at 2066 cm⁻¹. Vigorous bubbling of O₂ gave an acceptable yield of **1** up to 30%. This indicates that oxidation by O₂ is necessary for the formation of the Ir_2^{4+} core. The source of the CO in the Ir₂ complex is not clear yet.

Structure

An ORTEP[25] view of complex **2** is shown in Fig. 1 and selected distances and angles are summarized in Table 2. The two Ir atoms are bridged by two acetato ligands arranged in a *cis* geometry. The other equatorial sites on each Ir atom are occupied by a CO molecule and a Cl atom and the axial site is bonded by an MeCN molecule. The complex has a pseudo-C_2 axis across the bond between the two Ir atoms. The Ir atom and the co-ordinating atoms at the equatorial sites around it are arranged in a plane and the deviations of the atoms from the best plane are small: Ir(1) 0.00(3), Cl(1) 0.01(3), O(1) 0.03(3),

Table 1 Crystallographic data for [Ir$_2$(μ-O$_2$CMe)$_2$Cl$_2$(CO)$_2$(MeCN)$_2$] **2**, [Ir$_2$(μ-O$_2$CMe)$_2$Cl$_2$(CO)$_2$(dmso)$_2$] **3** and [Ir$_2$(μ-O$_2$CMe)$_2$Cl$_2$(CO)$_2$(py)$_2$] **4**

	2	**3**	**4**
Formula	C$_{10}$H$_{12}$Cl$_2$Ir$_2$N$_2$O$_6$	C$_{10}$H$_{18}$Cl$_2$Ir$_2$O$_8$S$_2$	C$_{16}$H$_{16}$Cl$_2$Ir$_2$N$_2$O$_6$
Formula weight	711.56	785.71	787.66
Crystal system	Orthorhombic	Triclinic	Monoclinic
Space group	$Pna2_1$ (no. 33)	$P\bar{1}$ (no. 2)	$C2/c$ (no. 15)
a/Å	15.681(1)	9.913(2)	16.3167(5)
b/Å	11.324(2)	12.268(2)	8.3925(5)
c/Å	9.807(1)	8.369(2)	16.0097(4)
$α$/°		90.57(1)	
$β$/°		95.88(2)	106.461(2)
$γ$/°		75.35(1)	
V/Å^3	1741.6(3)	979.3(3)	2102.5(1)
Z	4	2	4
T/°C	23	−80	23
$μ$(Mo-Kα)/cm^{-1}	156.40	141.30	129.69
Data, measured	2119	4744	3810
used	2119[a]	3922[b]	2082[b]
R_{int}	—	0.029	0.038
R, R'	0.070, 0.091	0.027, 0.032	0.030, 0.046

[a] All data. [b] With $I > 2σ(I)$.

Fig. 1 An ORTEP diagram of [Ir$_2$(μ-O$_2$CMe)$_2$Cl$_2$(CO)$_2$(MeCN)$_2$] **2** with 50% probability ellipsoids and hydrogen atoms omitted for clarity (as in all Figures).

Fig. 2 An ORTEP diagram of [Ir$_2$(μ-O$_2$CMe)$_2$Cl$_2$(CO)$_2$(dmso)$_2$] **3**.

Table 2 Selected bond distances (Å), angles (°) and torsion angles (°) for [Ir$_2$(μ-O$_2$CMe)$_2$Cl$_2$(CO)$_2$(MeCN)$_2$] **2** and [Ir$_2$(μ-O$_2$CMe)$_2$Cl$_2$(CO)$_2$-(dmso)$_2$] **3**

	2	**3**
Ir(1)–Ir(2)	2.569(1)	2.5980(5)
Ir(1)–Cl(1)	2.341(6)	2.323(2)
Ir(1)–O(1)	2.06(1)	2.066(4)
Ir(1)–O(3)	2.09(1)	2.081(4)
Ir(1)–Ax(1)[a]	2.18(2)	2.418(1)
Ir(1)–C(5)	1.82(2)	1.875(7)
Ir(2)–Cl(2)	2.335(5)	2.329(2)
Ir(2)–O(2)	2.07(2)	2.070(4)
Ir(2)–O(4)	2.05(1)	2.072(4)
Ir(2)–Ax(2)[a]	2.13(1)	2.426(2)
Ir(2)–C(6)	1.80(2)	1.868(7)
Ir(2)–Ir(1)–Ax(1)[a]	167.0(5)	168.77(4)
Ir(1)–Ir(2)–Ax(2)[a]	166.5(6)	169.16(4)
Cl(1)–Ir(1)–O(1)	175.2(4)	174.6(1)
O(3)–Ir(1)–C(5)	179.3(9)	178.5(2)
Cl(2)–Ir(2)–O(4)	174.3(6)	174.9(1)
O(2)–Ir(2)–C(6)	176.7(10)	178.4(2)
O(1)–Ir(1)–Ir(2)–O(2)	11.7(6)	16.2(2)
O(3)–Ir(1)–Ir(2)–O(4)	12.5(7)	16.2(2)

[a] Ax denotes an atom at an axial site: N for **2** and S for **3**.

O(3) 0.00(3) and C(5) 0.00(3) Å and Ir(2) 0.00(1), Cl(2) 0.01(1), O(2) 0.01(2), O(4) 0.07(2) and C(6) 0.01(2) Å. The dihedral angle between the two best planes is 16.6° and the planes are open toward the direction of the equatorial CO and Cl ligands. Each of the MeCN ligands is almost perpendicular to each of the best planes. Thus the Ir–NCMe bonds are bent from the Ir–Ir axis toward the middle of the two bridging acetato ligands. The bond angles Ir(2)–Ir(1)–N(1) and Ir(1)–Ir(2)–N(2) are 167.0(5) and 166.5(6)°, respectively. The equatorial ligands on an Ir atom are almost eclipsed with those on the neighboring metal atom: torsion angles O(1)–Ir(1)–Ir(2)–O(2) and O(3)–Ir(1)–Ir(2)–O(4) are 11.7(6) and 12.5(7)°, respectively.

The structures of complexes **3** and **4** are given in Figs. 2 and 3. The geometries of the Ir$_2$(μ-O$_2$CMe)$_2$Cl$_2$(CO)$_2$ core in **2**, **3** and **4** resemble each other. In the structure of **3** the axial dmso molecules are bonded by the S atom. Important bond distances and angles of **3** are summarized in Table 2 and those of **4** in Table 3. The axial ligands in complexes **3** and **4** are bent from the Ir–Ir axis toward the middle of the acetato bridges as in the geometry of **2**. This may have resulted from the dihedral angle between the planes of the equatorial ligands around each of the Ir atoms being open toward the equatorial Cl and CO groups and that the bond between the Ir atom and the axial ligand is perpendicular to the plane of the equatorial ligands.

The Ir–Ir distances in Ir$_2^{4+}$ complexes with π-conjugated bridging ligands such as carboxylate are listed in Table 4. The reported Ir–Ir distances are in the range between 2.524(3) Å in [Ir$_2$(μ-form)$_4$] (Hform = N,N'-di-p-tolylform-amidine)[12] and 2.695(2) Å in [Ir$_2$(μ-pyS)$_2$(CO)$_4$(CH$_2$I)I] (pySH = pyridine-2-thiol).[15] The Ir–Ir distances of the current [Ir$_2$(μ-O$_2$CMe)$_2$Cl$_2$(CO)$_2$L$_2$] complexes are similar to that of [Ir$_2$(μ-form)$_2$(MeCN)$_6$][BF$_4$]$_2$.[13]

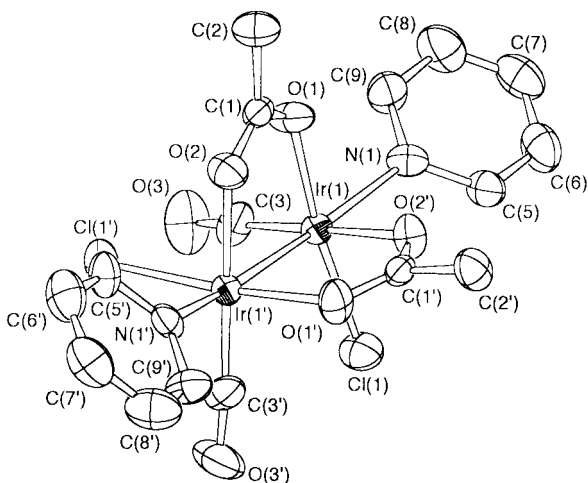**Fig. 3** An ORTEP diagram of $[Ir_2(\mu\text{-}O_2CMe)_2Cl_2(CO)_2(py)_2]$ **4**. One set of the disordered Cl and CO groups are omitted for clarity.

Table 3 Selected bond distances (Å), angles (°) and torsion angles (°) for $[Ir_2(\mu\text{-}O_2CMe)_2Cl_2(CO)_2(py)_2]$ **4** ^{a}

Ir(1)–Ir(1′)	2.5918(5)	Ir(1)–Cl(1)	2.299(5)
Ir(1)–Cl(2)	2.290(8)	Ir(1)–O(1)	2.063(5)
Ir(1)–O(2′)	2.076(6)	Ir(1)–N(1)	2.200(6)
Ir(1)–C(3)	1.81(2)	Ir(1)–C(4)	1.70(5)
Ir(1′)–Ir(1)–N(1)	165.9(2)	Cl(1)–Ir(1)–O(1)	172.6(2)
O(2)–Ir(1)–C(3)	179.1(6)	Cl(2)–Ir(1)–O(2′)	170.8(3)
O(1)–Ir(1)–C(4)	177(1)		
O(1)–Ir(1)–Ir(1′)–O(2)	7.0(2)		

^{a} $1 - x, y, \frac{1}{2} - z$.

Table 4 Ir–Ir distances (Å) in $Ir_2{}^{4+}$ complexes with anionic bridging ligands ^{a}

Complex	Distance	Ref.
$[Ir_2(\mu\text{-form})_4]$	2.524(3)	12
$[Ir_2(\mu\text{-}O_2CMe)_2Cl_2(CO)_2(MeCN)_2]$ **2**	2.569(1)	This work
$[Ir_2(\mu\text{-}O_2CMe)_2Cl_2(CO)_2(py)_2]$ **4**	2.5918(5)	This work
$[Ir_2(\mu\text{-}O_2CMe)_2Cl_2(CO)_2(dmso)_2]$ **3**	2.5980(5)	This work
$[Ir_2(\mu\text{-form})_2(MeCN)_6][BF_4]_2$	2.601(1)	13
$[Ir_2(\mu\text{-mbt})_2(CO)_4I_2]$	2.676(2)	16
$[Ir_2(\mu\text{-pyS})_2(CO)_4(CH_2I)I]$	2.695(2)	15

^{a} Hform = N,N'-Di-p-tolylformamidine, Hmbt = benzothiazole-2-thiol, pySH = pyridine-2-thiol.

Although a crystal structure analysis of complex **5** was carried out and the refinement gave a geometry similar to that of **4**, the results were of insufficient quality due to disorder in the arrangements of Cl atoms and CO groups and also in the orientation of the isopropyl groups. The assignment of the structure of **5** is supported by ^{1}H NMR, IR spectroscopy and elemental analysis.

Electrochemistry

The CV of complex **2** in MeCN is shown in Fig. 4(a). It exhibits a chemically reversible oxidation wave at 1.30 V (the potentials are *vs.* Fc$^+$–Fc). A chemically reversible oxidation response was observed for **4** and **5** in CH_2Cl_2 at $E_{1/2}$ of 0.97 and 0.94 V as shown in Fig. 4(b) and 4(c), respectively. Complex **3** did not show any redox response in the potential window of the dmso solution. No reduction wave was observed down to -1.5 V for the current complexes.

Bulk electrolysis of complex **4** at 1.25 V in 0.1 M Bu$^n_4$NPF$_6$–CH_2Cl_2 at 258 K gave a green solution. The electrolysed solution exhibited a quasi-reversible redox response at the potential
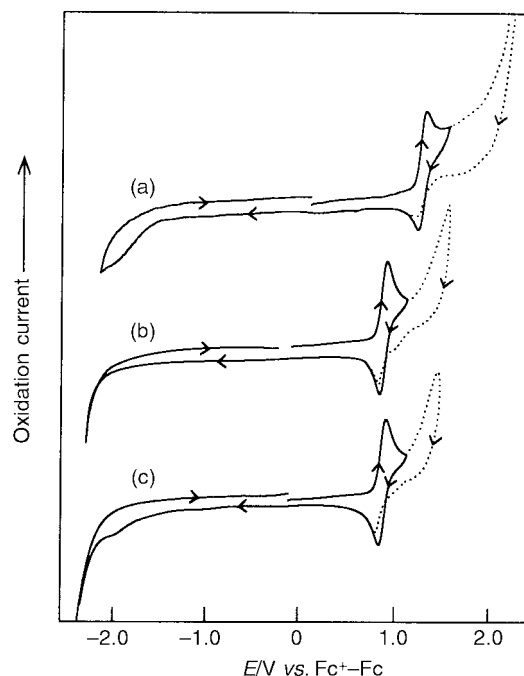
Fig. 4 CVs of (a) $[Ir_2(\mu\text{-}O_2CMe)_2Cl_2(CO)_2(MeCN)_2]$ **2** in MeCN, (b) $[Ir_2(\mu\text{-}O_2CMe)_2Cl_2(CO)_2(py)_2]$ **4** in CH_2Cl_2 and (c) $[Ir_2(\mu\text{-}O_2CMe)_2Cl_2(CO)_2(Pr^ipy)_2]$ **5** in CH_2Cl_2. The dotted lines represent the responses scanned beyond the $E^{ox}_{1/2}$ wave.

of 0.97 V, which is same as that for the oxidation of **4**. The consumed electricity showed that the oxidation is a one-electron transfer process. At room temperature the initially formed green color faded out in about 30 min and finally changed to yellow. The CV of the final yellow solution no longer showed the reversible wave at 0.97 V, indicating that the cationic radical of **4** is not stable at room temperature. A similar bulk electrolysis of **5** at 1.25 V at 258 K also gave a green solution of **5**$^{+•}$, which was also unstable at room temperature.

ESR of $[Ir_2(\mu\text{-}O_2CMe)_2Cl_2(CO)_2(py)_2]^{+•}$ 4$^{+•}$ and $[Ir_2\text{-}(\mu\text{-}O_2CMe)_2Cl_2(CO)_2(Pr^ipy)_2]^{+•}$ 5$^{+•}$

Owing to low stability of the cationic radicals of complexes **4** and **5**, we examined radiolytically generated **5**$^{+•}$ in a Freon mixture. The frozen Freon mixture is known to be an appropriate matrix for trapping cationic species formed upon radiolysis.[23,24] Since the same ESR spectrum was obtained by radiolysis of **5** at 77 K in a Freon mixture and by electrolysis of this complex at 258 K in CH_2Cl_2 as shown in Fig. 5(a) and 5(b), respectively, we can assign the spectra to **5**$^{+•}$. These spectra are axially symmetric and the principal values of the g tensor are $g_\perp = 2.51$ and $g_\parallel = 1.82$. Although the radiolysis of **4** could not be performed due to its low solubility in the Freon mixture, the paramagnetic species generated by its low-temperature electrolysis followed by freezing at 77 K gave the spectrum shown in Fig. 5(c). The spectrum is a rhombic one with the principal g values $g_1 = 2.62$, $g_2 = 2.49$ and $g_3 = 1.81$. The values of g_1 and g_2 are similar to the $g_\perp$ value of **5**$^{+•}$ and that of g_3 is similar to $g_\parallel$ of **5**$^{+•}$. Thus we can assign the spectrum of Fig. 5(c) to **4**$^{+•}$.

The large shifts of the principal values of the g tensors of complexes **4**$^{+•}$ and **5**$^{+•}$ from the free spin value ($g_e = 2.00$) show that their odd electron is distributed predominantly on the Ir atoms of which the valence-shell d orbitals have a large spin–orbit coupling constant. The absence of resolved hyperfine splitting due to the iridium nuclei in the spectra in Fig. 5 must be due to the smallness of the magnetic moment of this nucleus. The unique axis for their g tensors (axis 3 for **4**$^{+•}$ and the $\parallel$ axis for **5**$^{+•}$) must be the direction of the Ir–Ir bond.

The electronic configuration for the Ir–Ir bond in the current $Ir_2{}^{4+}$ complexes can be assumed to be $\sigma_{IrIr}{}^2\pi_{IrIr}{}^2\pi_{IrIr}{}'^2\delta_{IrIr}{}^2\pi_{IrIr}{}^{*2}$-
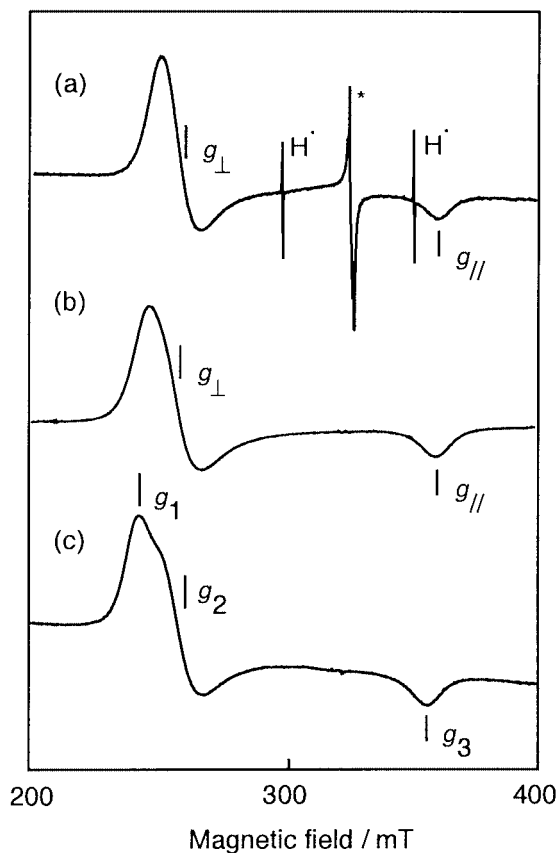
Fig. 5 X-Band ESR spectra of frozen solutions (77 K) of complex $5^{+•}$ generated (a) by radiolysis at 77 K in a Freon mixture and (b) by electrolysis at 258 K in CH_2Cl_2. (c) ESR spectrum at 77 K of $4^{+•}$ generated by electrolysis at 258 K in CH_2Cl_2. The signal with an asterisk in (a) is due to an unidentified species.

$\pi_{IrIr}*'^2\delta_{IrIr}*^2$ and candidates for the odd-electron orbital of $4^{+•}$ and $5^{+•}$ would be σ_{IrIr}, $\pi_{IrIr}*$ and $\delta_{IrIr}*$ orbitals in analogy to electronic structures of lantern-type $Rh_2{}^{4+}$ and $Rh_2{}^{5+}$ complexes.[2–6] Based on analyses on the g tensor of $Ir_2{}^{5+}$ complexes similar to those for $Rh_2{}^{5+}$ complexes[3] we expect its principal value for the direction parallel the Ir–Ir axis (g_{zz}) and the values for the directions perpendicular to the Ir–Ir axis (g_{xx} and g_{yy}) as follows: for $\delta_{IrIr}*$, $g_{zz} < g_e$ and $g_{xx} \approx g_{yy} > g_e$; for σ_{IrIr}, $g_{zz} \approx g_e$ and $g_{xx} \approx g_{yy} > g_e$; for $\pi_{IrIr}*$, $g_{zz} > g_e$. For the case of the $\pi_{IrIr}*$ odd-electron orbital the values of g_{xx} and g_{yy} need some comments. If the energy difference between the two $\pi_{IrIr}*$ orbitals is similar to or smaller than the one-electron spin–orbit coupling constant of the iridium 5d orbital, *ca.* 3000 cm^{-1},[26] the g tensor would be axially symmetric with $g_{xx} \approx g_{yy} > g_e$. If the energy difference is far larger than the one-electron spin–orbit coupling constant the g tensor would be rhombic and at least one of g_{xx} and g_{yy} would be less than g_e; this is due to the mixing of the d orbital component in an unoccupied molecular orbital σ antibonding between the metal atoms and the equatorial ligands into the $\pi_{IrIr}*$ odd-electron orbital through the spin–orbit coupling around the metal atoms. The observed g tensors of $4^{+•}$ and $5^{+•}$ are consistent with expectation for the state of the $\delta_{IrIr}*$ odd-electron orbital. The absence of hyperfine splitting arising from the ^{14}N nuclei is consistent with this electronic state. Thus we assign the odd-electron orbital of $4^{+•}$ and $5^{+•}$ to the $\delta_{IrIr}*$ orbital.

A recently reported study on an interesting $Ir_2{}^{6+}$ complex, $[Ir_2(hpp)_4Cl_2]$ (Hhpp = 1,3,4,6,7,8-hexahydro-2H-pyrimido-[1,2-*a*]pyrimidine), by Cotton and his co-workers[27] has shown that this complex with an idealized D_{4h} geometry has the open-shell configuration of $\sigma_{IrIr}{}^2\pi_{IrIr}{}^4\delta_{IrIr}{}^2\delta_{IrIr}*^2\pi_{IrIr}*^2$. The π-donating chloride ligands at the axial sites in Cotton's complex should have shifted the $\pi_{IrIr}*$ orbital upward in energy leaving the $\delta_{IrIr}*$ energy level unaffected because of the symmetry of the orbitals, whereas the equatorial chloride ligands in the current $4^{+•}$ and $5^{+•}$ complexes should have induced upward shifts of the energy levels of both of the $\delta_{IrIr}*$ and $\pi_{IrIr}*$ orbitals. The equatorial carbonyl ligands in the current complexes should have induced downward shifts in energies of both of the $\delta_{IrIr}*$ and $\pi_{IrIr}*$ orbitals, but this would not give much effect on the difference in their orbital energies. Thus we suppose the difference of the sites of the chloride ligands may be a source of the difference in the sequence of the energy levels of the $\pi_{IrIr}*$ and $\delta_{IrIr}*$ orbitals between Cotton's complex and $4^{+•}$ and $5^{+•}$.

References

1 F. A. Cotton and R. A. Walton, in *Multiple Bonds between Metal Atoms*, Oxford University Press, New York, 2nd edn., 1993, ch. 7, pp. 431–501.
2 T. Kawamura, K. Fukamachi and S. Hayashida, *J. Chem. Soc., Chem. Commun.*, 1979, 945.
3 T. Kawamura, K. Fukamachi, T. Sowa, S. Hayashida and T. Yonezawa, *J. Am. Chem. Soc.*, 1981, **103**, 364.
4 T. Sowa, T. Kawamura, T. Shida and T. Yonezawa, *Inorg. Chem.*, 1983, **22**, 56.
5 T. Kawamura, H. Katayama, H. Nishikawa and T. Yamabe, *J. Am. Chem. Soc.*, 1989, **111**, 8156.
6 T. Kawamura, M. Maeda, M. Miyamoto, H. Usami, K. Imaeda and M. Ebihara, *J. Am. Chem. Soc.*, 1998, **120**, 8136.
7 J. L. Atwood, K. A. Beveridge, G. W. Bushnell, K. R. Dixon, D. T. Eadie, S. R. Stobart and M. J. Zaworotko, *Inorg. Chem.*, 1984, **23**, 4050.
8 J. Powell, A. Kuksis, S. C. Nyburg and W. W. Ng, *Inorg. Chim. Acta*, 1982, **64**, L211.
9 M. A. Ciriano, A. R. Dias, P. M. Nunes, L. A. Oro, M. F. Minas da Piedade, M. E. Minas da Piedade, P. Ferreira da Silva, J. A. Martinho Simões, J. J. Pérez-Torrente and L. F. Veiros, *Struct. Chem.*, 1996, **7**, 337.
10 L. A. Oro, E. Sola, J. A. López, F. Torres, A. Elduque and F. J. Lahoz, *Inorg. Chem. Commun.*, 1998, **1**, 64.
11 C. Tejel, M. A. Ciriano, J. A. López, F. J. Lahoz and L. A. Oro, *Organometallics*, 1998, **17**, 1449.
12 F. A. Cotton and R. Poli, *Polyhedron*, 1987, **6**, 1625.
13 K. R. Dunbar, S. O. Majors and J. Sun, *Inorg. Chim. Acta*, 1995, **229**, 373.
14 F. A. Cotton and R. Poli, *Organometallics*, 1987, **6**, 1743.
15 M. A. Ciriano, F. Viguri, L. A. Oro, A. Tiripicchio and M. Tiripicchio-Camellini, *Angew. Chem., Int. Ed. Engl.*, 1987, **26**, 444.
16 M. A. Ciriano, S. Sebastián, L. A. Oro, A. Tiripicchio, M. Tiripicchio-Camellini and F. J. Lahoz, *Angew. Chem., Int. Ed. Engl.*, 1988, **27**, 402.
17 TEXSAN, Structure Analysis Package, Molecular Structure Corporation, Houston, TX, 1985.
18 D. T. Cromer and J. T. Waber, in *International Tables for X-Ray Crystallography*, Kynoch Press, Birmingham, 1974, vol. IV, Table 2.2A.
19 D. C. Creagh and W. J. McAuley, in *International Tables for X-Ray Crystallography*, ed. A. J. C. Wilson, Kluwer, Boston, 1992, vol. C, p. 219.
20 G. M. Sheldrick, in *Crystallographic Computing 3*, eds. G. M. Sheldrick, C. Kruger and R. Goddard, Oxford University Press, 1985, pp. 175–189.
21 N. Walker and D. Stuart, *Acta Crystallogr., Sect. A*, 1983, **39**, 158.
22 J. de Meulenaer and H. Tompa, *Acta Crystallogr.*, 1965, **19**, 1014.
23 T. Shida, Y. Nosaka and T. Kato, *J. Phys. Chem.*, 1978, **82**, 695.
24 A. Grimison and G. A. Simpson, *J. Phys. Chem.*, 1968, **72**, 1776.
25 C. K. Johnson, ORTEP II, Report ORNL-5138, Oak Ridge National Laboratory, Oak Ridge, TN, 1976.
26 B. A. Goodman and J. B. Raynor, *Adv. Inorg. Chem. Radiochem*, 1970, **13**, 135.
27 F. A. Cotton, C. A. Murillo and D. J. Timmons, *Chem. Commun.*, 1999, 1427.